ELSEVIER

Ocean Modelling 5 (2002) 65–76

Ocean Modelling

www.elsevier.com/locate/omodol

On aliasing Rossby waves induced by asynchronous time stepping

Rui Xin Huang *, Joseph Pedlosky

Department of Physical Oceanography, Woods Hole Oceanographic Institution, Woods Hole, MA 02543, USA

Received 7 February 2001; received in revised form 19 April 2002; accepted 25 April 2002

Abstract

The errors introduced by asynchronous time stepping are analyzed. It is shown that asynchronous time stepping distorts the structure and the speed of the lowest mode. For typical time step ratios used in climate simulations, the lowest mode is no longer a strictly barotropic mode, and the associated wave is much slower than the barotropic Rossby waves in the oceans. As a result, seasonal cycles simulated in model runs based on asynchronous time stepping are severely contaminated.

Keywords: Asynchronous time stepping; Rossby waves; Seasonal cycle; Oceanic general circulation model

1. Introduction

The asynchronous time stepping method has been widely used in OGCM experiments in order to speed up the computation. For example, for horizontal resolution of 1° or 2°, a time step on the order of hours is used for the velocity calculation, but a much longer time step, on the order of days, is used for the tracer calculation. In addition, the tracer time is used as the model time.

The justification and the consequence of asynchronous time stepping was discussed by Bryan (1984). His study was focused on the convergence to the equilibrium state, with particular emphasis on changes of the speed of the waves. With the recent trend of climate study, a more relevant question is how much such asynchronous time stepping can affect the climate variability on seasonal to inter-annual times scales. Danabasoglu et al. (1996) carried out a series of numerical experiments to find a practical way to spin up the oceanic circulation, by first using the

* Corresponding author.
E-mail address: rhuang@whoi.edu (R. Xin Huang).

1463-5003/02/$ - see front matter
PII: S1463-5003(02)00014-8

asynchronous time stepping and switching to the synchronous time stepping. According to their numerical experiments, they suggested that after a sufficient equilibrium state has been reached with asynchronous time steps, the model should be run with synchronous time step for 15 years in order to reach a synchronous equilibrium. Wang (2001) also discussed the distortion of the seasonal cycle when the asynchronous time stepping is used.

Despite the common practice of using the asynchronous time stepping in climate related studies, errors induced by such a technique remain unclear. Since most oceanic general circulation models of the new generation include the free surface elevation explicitly, accurately simulating the barotropic mode of the oceanic circulation is of vital importance. Thus, in this note we will focus on the issues related to the distortion of the physics associated with high frequency climate variability, including both the barotropic mode and the baroclinic modes.

2. Model formulation

The notion of using different time steps for different property equations can be shown to be equivalent to introducing an artificial small parameter, μ, which is the ratio of the short to the longer time steps. Thus, if we choose a short time step Δt_v for the velocity time step and Δt_ρ for the time step in the tracer equations, a new parameter $\mu = \Delta t_v/\Delta t_\rho$, usually small, implicitly alters the equations of motions. In this note we make its presence explicit and discuss the dynamical consequences of allowing $\mu \ll 1$. The equations are equivalent to the development in Bryan (1984) although he considered only free wave solutions.

For this purpose we consider the linearized form of the primitive equations describing the time evolution of large-scale motions forced by wind stress and buoyancy forcing. The governing equations are:

$$\frac{\partial u}{\partial t} = \mu\left(fv - \frac{1}{\rho_0}\frac{\partial p}{\partial x} + \frac{1}{\rho_0}\frac{\partial \tau^x}{\partial z}\right), \tag{1a}$$

$$\frac{\partial v}{\partial t} = \mu\left(- fu - \frac{1}{\rho_0}\frac{\partial p}{\partial y} + \frac{1}{\rho_0}\frac{\partial \tau^y}{\partial z}\right), \tag{1b}$$

$$0 = -\frac{\partial p}{\partial z} - \rho g, \tag{1c}$$

$$\frac{\partial u}{\partial x} + \frac{\partial v}{\partial y} + \frac{\partial w}{\partial z} = 0, \tag{1d}$$

$$\frac{\partial \rho}{\partial t} + w\frac{\partial \bar{\rho}}{\partial z} = -\rho_0 H, \tag{1e}$$

where $\mu \ll 1$ is a small parameter, H is a given function representing the applied buoyancy forcing and τ^x, τ^y are the components of the turbulent frictional stresses within the fluid. The fluid is contained between $z = 0$ and $z = -D$. Introducing the "compressed time",

$$\tau = \mu t, \tag{2}$$

the time-dependent equations become

$$\frac{\partial u}{\partial \tau} = fv - \frac{1}{\rho_0}\frac{\partial p}{\partial x} + \frac{1}{\rho_0}\frac{\partial \tau^x}{\partial z}, \tag{3a}$$

$$\frac{\partial v}{\partial \tau} = -fu - \frac{1}{\rho_0}\frac{\partial p}{\partial y} + \frac{1}{\rho_0}\frac{\partial \tau^y}{\partial z}, \tag{3b}$$

$$\mu\frac{\partial \rho}{\partial \tau} + w\frac{\partial \bar{\rho}}{\partial z} = -\rho_0 H. \tag{3c}$$

The boundary conditions are:

(1) At the free surface, $z = \eta$, $P = p/\rho_0 = 0$. A linearization of this condition to the fixed upper boundary $z = 0$ leads to

$$P = g\eta, \quad \text{or} \quad \mu P_\tau = gw \quad \text{at } z = 0. \tag{4a}$$

(2) At the bottom (assuming flat),

$$w = 0, \quad \text{at } z = -D. \tag{4b}$$

Using the hydrostatic relation (1c), these conditions are reduced to

$$\frac{\mu P_{z\tau}}{N^2} + \frac{P_\tau}{g} - \frac{gH}{N^2} = 0, \ z = 0, \tag{5a}$$

$$\frac{\mu P_{z\tau}}{N^2} - \frac{gH}{N^2} = 0, \ z = -D. \tag{5b}$$

We consider the solutions of Eqs. (3a)–(3c) for the case of a flat bottom ocean in the form of an eigenfunction expansion of the form:

$$[u, v, p/\rho_0] = \sum_n [U_n, V_n, g\eta_n]F_n(z), \tag{6a}$$

$$w = \sum_n W_n G_n(z), \tag{6b}$$

where the variables U_n, V_n, W_n, η_n are functions only of the horizontal coordinates. The eigenfunctions F_n and G_n satisfy:

$$\frac{\mathrm{d}}{\mathrm{d}z}\left(\frac{\mu}{N^2}\frac{\mathrm{d}F_n}{\mathrm{d}z}\right) + \frac{F_n}{gh_n} = 0, \tag{7a}$$

$$\frac{\mathrm{d}F_n}{\mathrm{d}z} = 0, \ z = -D, \tag{7b}$$

$$\frac{\mathrm{d}F_n}{\mathrm{d}z} + \frac{N^2}{\mu g}F_n = 0, \ z = 0. \tag{7c}$$

Note that the small parameter μ serves in the eigenvalue problem to artificially increase the magnitude of the buoyancy frequency. The nature of the eigenvalue problem for this vertical structure equation is such that for large enough N even the lowest mode, with F_1 independent of z for oceanographically reasonable values of N, will become strongly z dependent. Thus, a small enough value of μ can severely distort the eigenstructure of the barotropic mode and thus the projection on to it of the forcing. It will clearly also alter the eigenvalues, i.e., the equivalent depths, h_n and hence the propagation speed of all waves, particularly the barotropic mode.

The function G_n is related to F_n by the relations:

$$G_n = -\frac{\mu g}{N^2}\frac{\mathrm{d}F_n}{\mathrm{d}z}, \tag{8a}$$

$$F_n = h_n \frac{\mathrm{d}G_n}{\mathrm{d}z}. \tag{8b}$$

The density Eq. (3c) can be rewritten in terms of the pressure field through the aid of (1c), yielding, taking one further z derivative:

$$\frac{\partial}{\partial z}\left(\frac{\mu P_{z\tau}}{N^2}\right) + \frac{\partial w}{\partial z} = \frac{\partial}{\partial z}\left(\frac{gH}{N^2}\right). \tag{9}$$

If Eqs. (1d), (3a), (3b) and (9) are multiplied by the eigenfunction F_n and integrated over the depth of the fluid and use is made of the boundary conditions that w vanish at the bottom (5b) and the pressure vanishes at the free surface (5a), it can easily be shown that the resulting equations become:

$$\frac{\partial U_n}{\partial \tau} - fV_n = -g\frac{\partial \eta_n}{\partial x} + \tau_n^x, \tag{10a}$$

$$\frac{\partial V_n}{\partial \tau} + fU_n = -g\frac{\partial \eta_n}{\partial y} + \tau_n^y, \tag{10b}$$

$$\frac{\partial U_n}{\partial x} + \frac{\partial V_n}{\partial y} + \frac{W_n}{h_n} = 0, \tag{10c}$$

$$\frac{\partial \eta_n}{\partial \tau} - W_n = \frac{gh_n}{J_n}\int_{-D}^{0} \frac{\mathrm{d}F_n}{\mathrm{d}z}\frac{H}{N^2}\,\mathrm{d}z, \tag{10d}$$

where

$$J_n = \int_{-D}^{0} F_n^2\,\mathrm{d}z,$$

$$\frac{1}{\rho_0}\frac{\partial \vec{\tau}}{\partial z} = \sum_n \vec{\tau}_n F_n(z).$$

Thus, the equations take the form of the shallow water equations for a fluid with an equivalent depth h_n derived from the solution of (7a)–(7c). Note that the forcing in (10d) depends on the projection of the heating on the vertical derivative of the nth eigenfunction. For oceanographic realistic values of N, where the barotropic eigenfunction is independent of z this term would be zero. However, as shown below, for small enough value of μ, of the order of N^2D/g, this is no longer the case so that the asynchronous integrations, equivalent to small μ, will provide for an artificial forcing of the lowest mode, no longer z independent. Higher modes will also be affected but generally less so.

From the momentum equations the vorticity equation is obtained

$$\beta V_n + \mu\zeta_{n,\tau} = -f(U_{n,x} + V_{n,y}) + \mathrm{curl}\,\vec{\tau}_n, \tag{11}$$

where $\mathrm{curl}\,\vec{\tau}_n = (1/J_n)\int_{-D}^{0} \mathrm{curl}\,\vec{\tau}_z F_n\,\mathrm{d}z$.

For quasi-geostrophic motions on the β plane the τ derivatives and the variation of f from its constant value, as well as the direct effect of the wind stress are all negligible at lowest order in the momentum equations although they enter the vorticity balance. This allows the definition of a stream function,

$$\psi_n = g\eta_n/f_0. \tag{12}$$

If in addition we make the long wave approximation so that the relative vorticity can be ignored in (11):

$$\beta h_n V_n/f_0 = \frac{\beta h_n}{f_0}\frac{\partial \psi_n}{\partial x} = W_n + \operatorname{curl}\vec{\tau}_n. \tag{13}$$

For the barotropic mode the long wave approximation may be quantitatively in error due to the large external deformation radius. However, the basic distortion due to asynchronous stepping is quantitatively demonstrated with the long wave theory.

It follows that the evolution equation derived from (10d and 13) is now:

$$\begin{aligned} -\frac{f_0^2}{gh_n}\frac{\partial \psi_n}{\partial \tau} + \beta\frac{\partial \psi_n}{\partial x} &= -\frac{1}{J_n}\int_{-D}^{0}\frac{gf_0}{N^2}H\frac{\mathrm{d}F_n}{\mathrm{d}z}\,\mathrm{d}z + \frac{1}{\rho_0 J_n}\int_{-D}^{0}F_n\frac{\partial \operatorname{curl}\vec{\tau}}{\partial z}\,\mathrm{d}z \\ &= -\frac{1}{J_n}\int_{-D}^{0}\frac{gf_0}{N^2}H\frac{\mathrm{d}F_n}{\mathrm{d}z}\,\mathrm{d}z + \frac{1}{\rho_0 J_n}\int_{-D}^{0}\operatorname{curl}\vec{\tau}\frac{\mathrm{d}F_n}{\mathrm{d}z}\,\mathrm{d}z + \frac{1}{\rho_0 J_n}F_n(0)\operatorname{curl}\vec{\tau}(0). \end{aligned} \tag{14}$$

We note that the lowest mode, $n = 0$, is the "barotropic mode" and for moderate μ is essentially independent of z. In that case the principal forcing of the barotropic mode, from (14) must be the wind stress curl since all other forcing terms in (14) are proportional to the vertical derivative of F_0. As we shall see below, when μ is very small even the "barotropic" mode will have significant z dependence but it is still true that the major projection of the forcing on the lowest mode will be due to the wind stress curl. That being the case, it is natural to expect that the major error involved with the barotropic mode will be forced by the wind stress as the detailed numerical calculations presented below will demonstrate.

To illustrate the basic ideas we will discuss the simple case where N is constant. This simplification is especially apt since the major change in the modes occur near the upper boundary. The solution of the eigenproblem (7a)–(7c) is

$$F_n = \cos[m_n(z + D)] \tag{15}$$

with

$$m_n^2 = \frac{N^2/\mu}{gh_n} \tag{16}$$

which yields the eigenvalue relation

$$\tan(m_n D) = \frac{N^2 D/g}{(mD)\mu} \tag{17}$$

in terms of which the equivalent depth is given by:

$$gh_n = \frac{N^2/\mu}{m_n^2}. \tag{18a}$$

From (13) it is clear that the speed of propagation in τ units is given by

$$c_{n,\mu} = \frac{\beta g h_{n,\mu}}{f_0^2} = c_{n,1}\frac{h_{n,\mu}}{h_{n,1}} = \frac{\beta N^2/\mu}{f_0^2 m_n^2}, \tag{18b}$$

where the subscript (n,μ) and $(n,1)$ indicate the nth mode for the case with μ arbitrary but normally $\ll 1$ and $\mu = 1$.

In the ocean $(N^2D/g) = -(D/\rho_0 \partial z/\partial \rho) \ll 1$. When $\mu = 1$, i.e., for the case of synchronous time stepping, the first mode, or the lowest mode, has a vertical structure that is almost independent of depth, and it is thus called the barotropic mode. The solution for (17) is $m_{1,1} \approx N/\sqrt{gD}$. Thus, the equivalent depth is $h_{1,1} \approx D$. Since $m_{1,1}D \ll 1$, the eigenfunction $F_1 = \cos[m_{1,1}D(1+z/D)]$ is essentially constant in z. For small μ, the lowest eigenvalue increases with decreasing μ finally asymptoting to $\pi/2$.

Since $h_{1,1} \approx D$, the speed of the first mode in the oceans is

$$c_{1,1} = \frac{\beta g D}{f_0^2}. \tag{19}$$

Since $N^2D/g \ll 1$, for the case of $\mu \geqslant N^2D/g$ the solution of (17) is

$$m_{1,\mu}^2 \approx \frac{N^2}{\mu g D}, \tag{20}$$

$$h_{1,\mu} \approx \mu D = \mu h_{1,1}, \tag{21}$$

$$c_{n,\mu} \approx c_{n,1}. \tag{22}$$

Recall the speed defined above is for the "compressed" time τ, and the real speed in the normal time t is

$$C_{1,\mu} = \frac{\mathrm{d}x}{\mathrm{d}t} = \mu\left(\frac{\mathrm{d}x}{\mathrm{d}\tau}\right)_\mu = \mu c_{1,\mu} \approx \mu C_{1,1}. \tag{23}$$

Therefore, the lowest mode propagates with a speed much smaller than that of the standard barotropic Rossby waves.

On the other hand, as long as $\mu \approx \geqslant N^2D/g$, the eigenvalues for higher modes ($m > 1$) are essentially constant, plus a small correction term that is proportional to μ, Table 1. As a result, the speed of the higher baroclinic modes in the case of asynchronous stepping is only slightly slower than that of synchronous time stepping.

We consider the case with forcing due to wind stress and surface trapped buoyancy forcing that is switched on and remains constant thereafter. If (14) is solved in the region $x \leqslant x_e$, the solution breaks into two parts:

(1) For $x \leqslant x_e - C_n t$

$$\psi_n = \Psi_n^s(x,y) - \Psi_n^s(x + C_n t, y), \tag{24}$$

Table 1
Eigenvalues of the first three modes for the case of $N^2D/g = 0.002$

$1/\mu$	1.0	10	20	30	40	50	70	100
mD_1	0.04471	0.14095	0.19867	0.24253	0.27913	0.31105	0.36566	0.43284
$mD_2 - \pi$	0.00064	0.00635	0.01268	0.01898	0.02526	0.03150	0.04392	0.06234
$mD_3 - 2\pi$	0.00032	0.00318	0.00636	0.00953	0.01271	0.01587	0.02220	0.03166

where the steady solution is

$$\Psi_n^s = -\frac{1}{\beta\rho_0}\int_x^{x_e} \Theta_n(x')\,dx', \tag{25a}$$

$$\Theta_n = \frac{1}{J_n}\int_{-D}^{0} \frac{gf_0}{N^2}\frac{\partial F_n}{\partial z} H\,dz - \frac{1}{\rho_0 J_n}\int_{-D}^{0} \mathrm{curl}\,\vec{\tau}\frac{dF_n}{dz}\,dz + \frac{1}{\rho_0 J_n}F_n(0)\mathrm{curl}\,\vec{\tau}(0). \tag{25b}$$

For convenience we will also use a standardized amplitude function

$$\theta_n = \frac{N^2}{gf_0}\Theta_n. \tag{26}$$

(2) For $x \geqslant x_e - C_n t$

$$\psi_n = \psi_n^s. \tag{27}$$

For climate study, the tracer time step is about 20–100 times larger than the velocity time step. As an example, the structure of the first and second eigenfunctions for the case when $N^2D/g = 0.002$, $\mu = 0.001$ and $\mu = 0.05$ are shown in Figs. 1 and 2. It is clear that the first mode is no longer a strict barotropic mode, and the second mode is no longer a strictly baroclinic mode although for $\mu = 0.05$ the changes are small. Consequently, for the same surface-trapped buoyancy forcing, using the asynchronous time stepping the projection onto the first mode will be much larger than that for the synchronous time stepping.

To illustrate the idea, we choose a surface-trapped step function for the buoyancy forcing with no wind stress

$$H = 1 \quad 0 \leqslant z \leqslant -d,$$

$$H = 0 \quad -d < z \leqslant -D,$$

where $d = 0.1D$. As the ratio of time steps $1/\mu$ increases, the ratio of the speed of the first mode increases, closely following the rule in (22). At the same time, the projection onto the first mode increases in proportion, but the projection onto higher modes decline, Fig. 3.

Note that for very small μ as shown in Fig. 1 the lowest mode for F now is strongly z dependent while for only moderately small μ, as shown in Fig. 2, the mode remains essentially z independent,

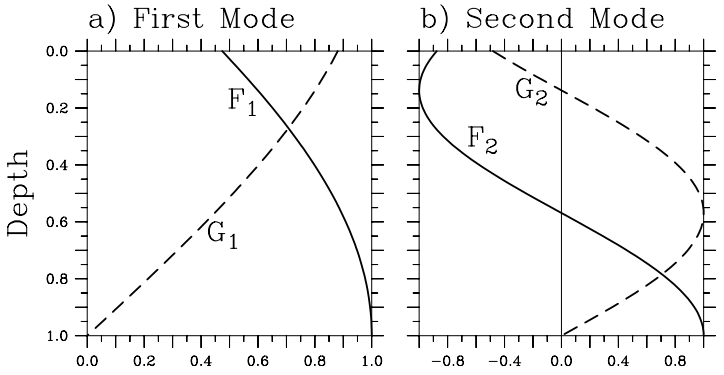

Fig. 1. Structure of the first and second eigenfunctions for the case of $N^2D/g = 0.002$ and $\mu = 0.001$.

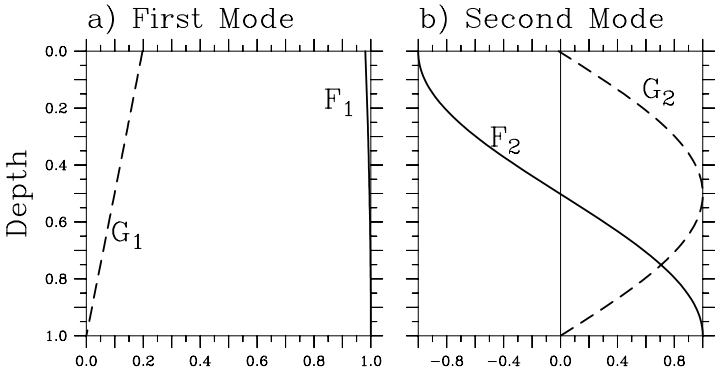

Fig. 2. Structure of the first and second eigenfunctions for the case of $N^2D/g = 0.002$ and $\mu = 0.05$.

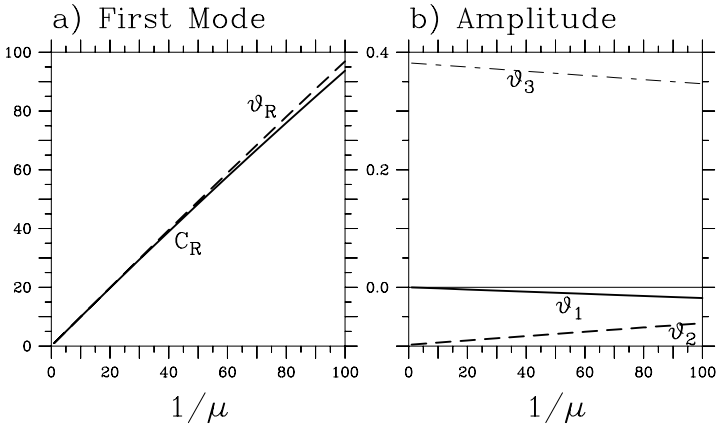

Fig. 3. (a) Relative amplitude $\theta_R = \theta_{1,1}/\theta_{1,\mu}$ and relative speed $C_R = C_{1,1}/C_{1,\mu}$ of the first mode as functions of the time step ratio $1/\mu$. (b) Amplitude of the first three modes, θ_n, as functions of the time step ratio λ.

i.e., barotropic in structure. We therefore expect, in the latter case, that the major forcing of the lowest mode will be due to the wind stress.

3. Application to an oceanic general circulation model

We have carried out numerical experiments to test the basic idea, using a newly developed oceanic circulation model, the pressure coordinate ocean model, based on the pressure-sigma coordinates (Huang et al., 2001). This new model is a truly non-Boussinesq model, so it can simulate the time evolution of the circulation much more accurately.

The model ocean is a square basin covering from the Equator to 60° N, and 60° wide. The model basin was at rest initially and the initial temperature was the global mean potential temperature obtained from Da Silva et al. (1994) climatology and salinity was 35. The model ocean is 4000 m deep, and it has 15 layers. The potential temperature at the top and bottom of the model ocean are 13.62° and 1.01° respectively, and the difference in potential density is 1.80 σ-unit, so

$N^2D/g = 0.0018$, which is quite close to the value of 0.002 used in the discussion above. The time step for the velocity is 1.2 h, and the time step for the temperature is 24 h, thus $\mu = 0.05$.

In the first experiment, the ocean is driven by the wind stress only. Wind stress is taken as the climatological zonally mean zonal wind stress, plus a seasonal cycle whose amplitude is 30% of the annual mean wind stress, i.e., $\tau^x = (1.0 + 0.3\sin\omega t)\tau_0^x$, where ω corresponds to an annual frequency and τ_0^x is the climatological zonally mean zonal wind stress. Furthermore, the wind stress is imposed for three grids next to the eastern boundary, so away from the eastern boundary the ocean is force-free and the Rossby waves diagnosed there should be the free Rossby waves. The model was run, using both the synchronous and asynchronous time stepping. The errors induced by the asynchronous time stepping propagate with two speeds, as shown in Fig. 4. At this latitude, the undistorted barotropic Rossby waves take about one week to cross the basin of 60° wide. The fast speed of the errors propagation corresponds to a value of 60°/140 days, so it is roughly 20 times slower than the undistorted barotropic waves.

Note that phase speed of the Rossby waves discussed above applies to long waves, and these take about 0.5 day to cross the basin at 30° N. Of course, for the long waves the phase speed and group velocity are the same. On the other hand, the corresponding group velocity for short waves is

$$c_{g,x} = -\frac{\beta\left(l^2 + \frac{f^2}{gD} - k^2\right)}{\left(k^2 + l^2 + \frac{f^2}{gD}\right)^2}.$$

The experiment was driven by the zonal-mean wind stress averaged over the global oceans which has a wave length in the meridional direction of about 4500 km. Since the wind stress is localized near the eastern boundary, it will excite all x wave numbers. However, the $k = 0$ contribution will correspond to the signal crossing the basin fastest and it will take 7 days to cross the basin.

As discussed above, the projection of the perturbation onto the second mode in the case of asynchronous time stepping is also different from the case of synchronous time stepping. As listed in Table 2, the standard projection function onto the second mode is -0.0975 for the case of $\mu = 1$, while it is -0.0904 for the case of $\mu = 0.05$. In addition, the the speed of the undistorted and distorted second modes are slightly different, with a ratio of 0.992. With the difference in

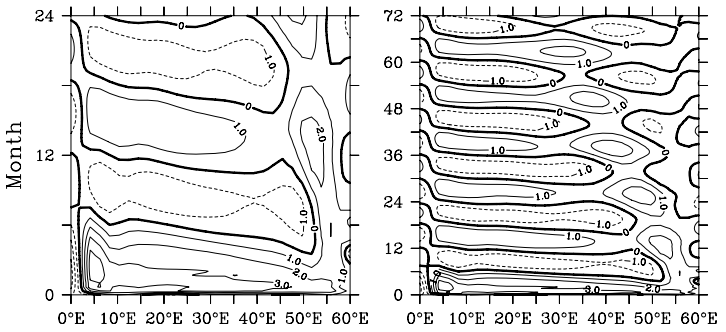

Fig. 4. The errors of the sea surface elevation induced by asynchronous time stepping, taking along a section at 30° N, in mm.

Table 2
Comparison for the projections onto the first and second modes for the case of $\mu = 0.05$

μ	$F_1(0)$	$F_2(0)$	$G_1(0)$	$G_2(0)$	$c_{1,\mu}/c_{1,1}$	$c_{2,\mu}/c_{2,1}$	θ_1	θ_2
1.0	0.9990	−1.00000	0.04469	−0.00064	1.0	1.0	c−0.00019	−0.0975
0.05	0.9803	−0.99992	0.19737	−0.01268	0.0506	0.992	−0.00378	−0.0904

amplitude and phase speed, a simple initial value problem can be set up similar to the example of the previous section and it demonstrates that substantial errors can be induced along the wave pathway. As shown in Fig. 4b, there is indeed a group of wave packages due to the error induced by the asynchronous time stepping that propagate westward with a speed of about 60°/12 years, corresponding to the first baroclinic Rossby waves. The results from this experiment indicates that using asynchronous time stepping to study climate variability for annual to decadal times scales may induce substantial distortions to the solutions.

The errors in the sea surface elevation are also compared with the free surface elevation and its annual cycle, removing the trend by moving averaging over one-year window, Fig. 5. Since errors have the same amplitude as the seasonal cycle, they are not acceptable. Note that the errors are roughly half year out of phase, compared with the signals. The baroclinic signals arrive this station after year 3, and the thermocline (which can be seen from the sharp increase of the free surface elevation) is gradually established after the passing of the first baroclinic Rossby waves. Although the amplitude of the seasonal cycle remains roughly unchanged, the errors are noticeably large as the first baroclinic waves pass through this station between year 4 and year 6. After the passage of the first baroclinic waves, the amplitude of the errors is reduced to the previous level.

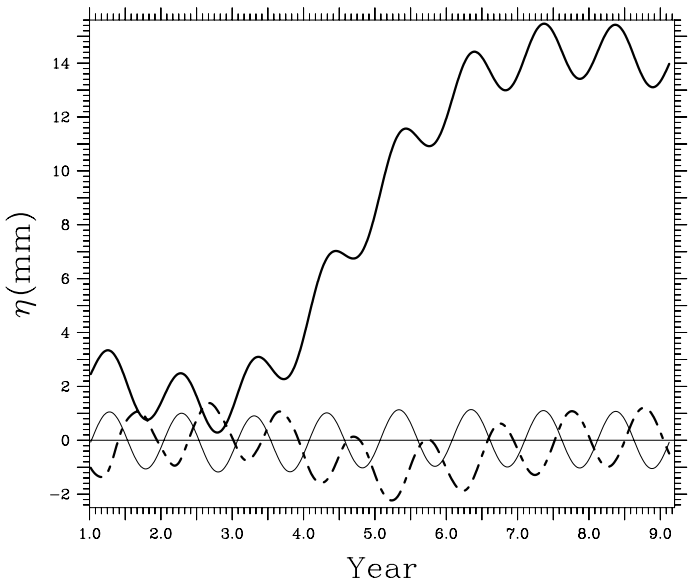

Fig. 5. Free surface elevation (heavy line), the seasonal cycle (thin line) and the errors induced by asynchronous time stepping (dashed line), taking at a station at the center of the basin (30° E, 30° N).

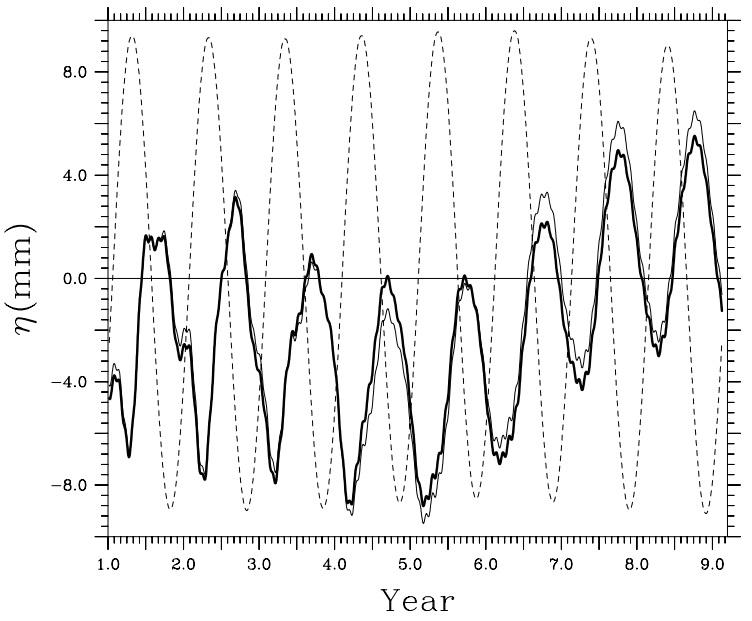

Fig. 6. Errors in the free surface elevation induce by asynchronous time stepping for the case with wind stress only (heavy line), the seasonal cycle (thin dashed line) and the errors induced by asynchronous time stepping driven by both wind stress and thermal relaxation (thin line), taking at a station at the center of the basin (10° E, 30° N).

In the second experiment, the ocean is driven by the same zonal wind stress; however, the whole basin is forced by the wind stress. In the third experiment, thermal forcing is added: the sea surface of the model ocean is relaxed to the reference temperature that includes the seasonal cycle $T_r = T_{r,0} + \Delta T_r(y) \sin \omega t$, where $T_{r,0}$ is the zonally mean sea surface temperature from Da Silva et al. (1994) climatology, $\Delta T_r(y) = 2.0 + 3.0 \times \phi/\Delta\phi$, ($\Delta\phi = 60°$).

In this case the error induced by the wind-forcing case is much larger than the previous experiment because the whole basin is subject to the wind stress forcing; however, adding the thermal forcing anomaly does not change the errors much, Fig. 6. Thus, errors induced by the buoyancy forcing are relatively small for a small μ. As seen from Fig. 6, errors in the free surface elevation have the same amplitude as the seasonal cycle of the free surface itself; thus, the seasonal cycle of the model ocean is severely contaminated.

Acknowledgements

We thank for Xiangze Jin's help in running the numerical experiments using the oceanic general circulation model. RXH was supported by National Science Foundation through grant OCE-0094807 to the Woods Hole Oceanographic Institution. JP was supported by National Science Foundation through grant OCE-9301845 to the Woods Hole Oceanographic Institution. Woods Hole Contribution #10423.

References

Bryan, K., 1984. Accelerating the convergence to equilibrium of ocean-climate models. J. Phys. Oceanogr. 14, 666–673.

Danabasoglu, G., McWilliams, Large, W.G., 1996. Approach to equilibrium in accelerated global oceanic models. J. Climate 9, 1092–1110.

Da Silva, A.M., Young, C.C., Levitus, S., 1994. Atlas of surface marine 1: Algorithms and procedures. U.S. Dept. of Commerce. Washington, DC.

Huang, R.X., Jin, X.-Z., Zhang, X.-H., 2001. A oceanic general circulation model in pressure coordinates. Adv. Atmos. Sci. 18, 1–22.

Wang, D., 2001. A note on using the accelerated convergence method in climate models. Tellus 53A, 27–34.